CISK–rossby wave and the 30–60 Day Oscillation in the Tropics

Liao Qinghai (廖清海) and *Li Chongyin* (李崇银)
Institute of Atmospheric Physics, Chinese Academy of Sciences, Beijing 100029
Received April 19, 1994; revised July 15, 1994

ABSTRACT

The 30–60 day oscillation is an important aspect of the atmospheric variance in the tropical area. A number of works have been done on this phenomenon, this article is a further one. A quasi–geostrophic linear model that consists of a two–layer free atmosphere and a well–mixed boundary layer is used to investigate the instability of intraseasonal oscillation, its propagation and vertical structures. Results show that the dynamical coupling and interaction between the barotropic and baroclinic components via boundary layer convergence / divergence are responsible for the appearance of a new kind of low–frequency wave. Such wave is very different from the traditional tropical Rossby wave. It can propagate westward and eastward. Some behaviours of it appear to resemble the observed 30–60 day oscillation mode in many aspects, such as vertical structures, zonal and meridional propagations. Now many researchers emphasize the direct relationship between CISK–Kelvin mode and the tropical atmospheric 30–60 oscillation. It is considered that CISK–Rossby mode should not be neglected.

Key words: *CISK–Rossby wave, 30–60 day oscillation in the tropics*

I. INTRODUCTION

The 30–60 day oscillation was first identified by Madden and Julian (1971, 1972) 20 years ago, using zonal wind and surface pressure data in the tropical atmosphere. They suggested that the oscillation refers largely to a wavenumber 1 zonal wind perturbation which propagates slowly eastward, and originated from the tropical Indian and the Western Pacific. In recent years, some general characteristics of the phenomenon have been extensively documented in terms of OLR and divergent circulation. The 30–60 day oscillation slowly propagates northward and eastward with zonal phase speed about 10 ms^{-1} and meridional speed 1–3ms^{-1}. The upper tropospheric zonal winds are almost out of phase with lower ones. The zonal circulation mainly shows wavenumber 1 pattern. The 30–60 day oscillation has obvious two–dimensional Rossby wave train pattern which indicates the feature of energy dispersion. It has been further noticed that 30–60 day oscillation disturbance sometimes propagates westward and southward (Knutson and Weickman, 1986). The above general features of the 30–60 day oscillation have been simulated more and more using various versions of numerical models(Hayashi and Sumi, 1986; Lau and Peng,1987; Swinbank et al,1988;Hendon,1988). However, the simulated phase speed tends to be greater than the observed. In order to further understand the activities and excitement mechanism of the 30–60 day oscillation, dynamical studies are needed. Now, they are becoming more and more important. Chang (1977) studied the tropical atmospheric motion with cumulus frictions and Newtonian cooling, and suggested that cumulus convective heating is related to the low frequency oscillation. Li(1985) first introduced the wave–CISK mechanism to explain the 30–60 day oscillation of the monsoon troughs in South Asia. Lau and Peng (1987) indicated that the eastward propagation

of the intraseasonal oscillation in the tropical atmosphere arises as the so-called "mobile wave-CISK" mechanism.By way of this mechanism, the heat source feeds on the intrinsic equatorial waves, and Kelvin wave is selectively amplified, which in turn causes the heat source to propagate eastward. However, the phase speed of the propagation is much faster than the observed. In order to solve this problem, Takahashi (1987) further investigated the effects of the vertical heating profile. He showed that the model phase speed is consistent with that of observed if the shape of heating profile is adaptable. Wang (1988) pointed out that moist Kelvin wave can be related to the intraseasonal disturbance. These studies all pay their attention to Kelvin wave with CISK, thus may be called "CISK-Kelvin wave" theory. Although such theory can explain some features of the tropical atmospheric 30-60 day oscillation,especially its eastward propagation,it is difficult to describe the others such as westward propagation, two-dimensional Rossby wave train characteristic of the oscillation, and the couple between zonal winds in the equatorial area and wind system in subtropical area(Hendon, 1988; Rui and Wang, 1990). It is well known that Kelvin mode decays rapidly in meridional direction. This property prevents it from finding the keys to these problems. Further dynamical exploration is needed. Li (1990) proposed that a so-called CISK-Rossby wave theory in the tropical area away from the equator. It is believed that CISK-Rossby wave arises from the cumulus convective feedback, It can either propagates westward or eastward, and its phase speed is consistent with the observed. Meanwhile, this Rossby wave is dispersive, which explains the two-dimensional Rossby wave train feature of the oscillation. Liu (1990) proved the existence of CISK-Rossby wave in analytical way, but their two-way propagating CISK-Rossby and CISK-Kelvin waves are all stable on their propagation way. This is inconsistent with the observed no decaying or even intensifying propagation.

Our main objects of this article are to examine the properties of CISK-Rossby wave in the tropical atmosphere and relate them to low frequency oscillation.

II. MODEL AND ITS SOLUTIONS

The atmosphere is taken as Boussinesq fluid.For low-frequency oscillation, the characteristic scale (30-60 days) is much greater than $(2\Omega\sin\varphi)^{-1}$, the inertial time scale. A higher accuracy approximation than quasi-geostrophic approximation is introduced to filter out high frequency inertial-gravity wave, the mixed Rossby-gravity wave. This approximation was first developed by Anderson and Gill (1972). Basic equations governing low-frequency perturbation motions can be written:

$$fU = -\Phi_y - \frac{1}{f}\Phi_{xt} - \frac{\beta}{f}\Phi, \tag{1}$$

$$fV = \Phi_x - \frac{1}{f}\Phi_{yt}, \tag{2}$$

$$U_x + V_y + W_z = 0, \tag{3}$$

$$\Phi_{tz} + N^2 W = \eta N^2 W_B, \tag{4}$$

where U and V are velocities in x and y directions, respectively; Φ is the perturbed potential height at certain layer; $f=\beta y$ is the Coriolis parameter; N^2 the static stability parameter, about $10^{-4}s^{-1}$; W the vertical velocity; W_B the vertical velocity at the top of mixed boundary layer; $\eta(z)$ is the nondimensional parameter,measuring the rate of condensation.

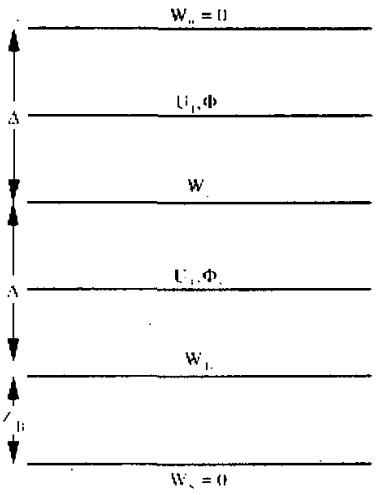

Fig. 1. Schematic vertical structure of the model.

The atmosphere is divided into $2\frac{1}{2}$ layers as Fig. 1 illustrated, which consists of a two-level representation of the free atmosphere and a well-mixed boundary layer. Writing U, V, and Φ at levels 1 and 3 and W at level 2, then substitute Eqs.(1)–(2) into Eq.(3)

$$\left(\frac{\partial^2}{\partial x^2}+\frac{\partial^2}{\partial y^2}\right)\Phi_t+\beta\Phi_x-f^2W_z=0. \tag{5}$$

Writing Eq.(5) at levels 1 and 3 and Eq.(4) at level 2, and assuming the velocity at the top of the troposhere $W=0$, then we have

$$\left(\frac{\partial^2}{\partial x^2}+\frac{\partial^2}{\partial y^2}\right)\Phi_{1t}+\beta\Phi_{1x}-f^2\frac{0-W_2}{\triangle}=0, \tag{6}$$

$$\left(\frac{\partial^2}{\partial x^2}+\frac{\partial^2}{\partial y^2}\right)\Phi_{3t}+\beta\Phi_{3x}-f^2\frac{W_2-W_B}{\triangle}=0, \tag{7}$$

$$\frac{\partial}{\partial t}\left(\frac{\Phi_1-\Phi_3}{\triangle}\right)+N^2W_2=\eta_2(z)N^2W_B. \tag{8}$$

Introducing barotropic and baroclinic parts of wind and geopotential defined by

$$\left.\begin{aligned}\overline{U}&=\frac{1}{2}(U_1+U_3) & \tilde{U}&=\frac{1}{2}(U_1-U_3)\\ \overline{V}&=\frac{1}{2}(V_1+V_3) & \tilde{V}&=\frac{1}{2}(V_1-V_3)\\ \overline{\Phi}&=\frac{1}{2}(\Phi_1+\Phi_3) & \tilde{\Phi}&=\frac{1}{2}(\Phi_1-\Phi_3)\end{aligned}\right\}, \tag{9}$$

we have

$$\left(\frac{\partial^2}{\partial x^2}+\frac{\partial^2}{\partial y^2}\right)\overline{\Phi}_t+\beta\overline{\Phi}_x+f^2\frac{W_B}{2\triangle}=0, \tag{10}$$

$$\left(\frac{\partial^2}{\partial x^2}+\frac{\partial^2}{\partial y^2}\right)\tilde{\Phi}_t+\beta\tilde{\Phi}_x+f^2\frac{2W_2-W_B}{2\triangle}=0, \tag{11}$$

$$\frac{\partial}{\partial t}\tilde{\Phi}+\frac{1}{2}\triangle N^2 W_2=\frac{1}{2}\triangle\eta_2 N^2 W_B \tag{12}$$

From Eq.(11) with the aid of Eq.(12), we obtain

$$\left(\frac{\partial^2}{\partial x^2}+\frac{\partial^2}{\partial y^2}-\frac{f^2}{C_a^2}\right)\tilde{\Phi}_t+\beta\tilde{\Phi}_x=\left(\frac{1}{2}-\eta_2\right)\frac{f^2}{\triangle}W_B, \tag{13}$$

where $Ca^2=\frac{1}{2}\Delta^2 N^2=(49\mathrm{m/s})^2$. Eqs.(10)–(13) are the governing sets for the free atmosphere, and W_B is the vertical velocity at the top of boundary layer. To evaluate W_B, we introduce perturbation equations for a steady, barotropic, well-mixed boundary layer, and write them as

$$K_m U_B-fV_B+\Phi_{Bx}=0, \tag{14}$$

$$fU_B+K_B V_B+\Phi_{By}=0, \tag{15}$$

$$W_B=-Z_B(U_{Bx}+V_{By}), \tag{16}$$

where subscript "B" denotes boundary layer variables; U_B and V_B are the averages of the boundary zonal and meridional winds respectively, Z_B is the averaged height of the top of boundary layer. In derivation of Eqs.(14)–(16), we have assumed that the surface stress is proportional to the transport of mass in the boundary layer, and the proportional rate Km is a constant in the following calculation; Φ_B is the geopotential at the boundary layer, taken as Φ_3.

From Eqs(14)–(16), we obtain

$$f^2 W_B=Z_B\left(\beta\Phi_{3x}+K_m\left(\frac{\partial^2}{\partial x^2}+\frac{\partial^2}{\partial y^2}\right)\Phi_3\right) \tag{17}$$

Substituting of Eq.(17) into Eq.(10) and Eq.(13) yeilds

$$\left(\frac{\partial^2}{\partial x^2}+\frac{\partial^2}{\partial y^2}\right)\bar{\Phi}_t+\beta\bar{\Phi}_x+\frac{Z_B}{2\triangle}\left(\beta\bar{\Phi}_x+K_m\nabla^2\bar{\Phi}\right)$$
$$=\frac{Z_B}{2\triangle}(\beta\tilde{\Phi}_x+K_m\left(\frac{\partial^2}{\partial x^2}+\frac{\partial^2}{\partial y^2}\right)\tilde{\Phi}), \tag{18}$$

$$\left(\frac{\partial^2}{\partial x^2}+\frac{\partial^2}{\partial y^2}-\frac{f^2}{C_a^2}\right)\tilde{\Phi}_t+\beta\tilde{\Phi}_x+\frac{(1-2\eta_2)Z_B}{2\triangle}\left(\beta\tilde{\Phi}_x+K_m\left(\frac{\partial^2}{\partial x^2}+\frac{\partial^2}{\partial y^2}\right)\tilde{\Phi}\right)$$
$$=\frac{(1-2\eta_2)Z_B}{2\triangle}\left(\beta\bar{\Phi}_x+K_m\left(\frac{\partial^2}{\partial x^2}+\frac{\partial^2}{\partial y^2}\right)\bar{\Phi}\right) \tag{19}$$

Eqs.(18)–(19) are the coupled atmospheric motion sets which represent the interaction between baroclinic modes and barotropic modes via tropical boundary layer.

Using the time scale $T=(2\beta Ca)^{\frac{1}{2}}$, the horizonal length scale $L=(Ca/2\beta)^{1/2}$, the geopotential scale Ca^2, the vertical velocity scale $2\Delta T^{-1}$, and writing $Z_B/\Delta=d$, $f=\beta y$, $\beta=2.3\times10^{-11}\mathrm{m^{-1}s^{-1}}$, we obtain nondimensional forms of Eqs.(18) and (19)

$$\nabla^2\bar{\Phi}_t+\frac{1}{2}\bar{\Phi}_x+\frac{d}{4}\left(\bar{\Phi}_x+K'_m\left(\frac{\partial^2}{\partial x^2}+\frac{\partial^2}{\partial y^2}\right)\bar{\Phi}\right)$$
$$=\frac{d}{4}\left(\tilde{\Phi}_x+K_m\nabla^2\tilde{\Phi}\right), \tag{20}$$
$$\left(\frac{\partial^2}{\partial x^2}+\frac{\partial^2}{\partial y^2}-\frac{y^2}{4}\right)\tilde{\Phi}_x+\frac{1}{2}\tilde{\Phi}_x+\frac{(1-2\eta_2)d}{4}\left(\tilde{\Phi}_x+K_m\left(\frac{\partial^2}{\partial x^2}+\frac{\partial^2}{\partial y^2}\right)\tilde{\Phi}\right)$$
$$=\frac{(1-2\eta_2)d}{4}\left(\bar{\Phi}_x+K'_m\left(\frac{\partial^2}{\partial x^2}+\frac{\partial^2}{\partial y^2}\right)\bar{\Phi}\right), \tag{21}$$

where $K'_m=2K_mT$. Solutions to Eqs.(20) and (21) are sought of the form

$$(\bar{\Phi}_n,\tilde{\Phi}_n)=\sum_{n=0}^{\infty}(\bar{\Phi}_n,\ \tilde{\Phi}_n)D_n(y)e^{i(kx-\sigma t)}$$

Substituting them into Eqs.(20) and (21) yeilds

$$\sum_{n=0}^{\infty}i\sigma\left(k^2+n+\frac{1}{2}\right)\tilde{\Phi}_nD_n(y)$$
$$+\sum_{n=0}^{\infty}\left\{\frac{1}{2}ik\left[1+\frac{(1-2\eta_2)d}{2}\right]-\frac{(1-2\eta_2)d}{4}\left(k^2+\frac{2n+1}{4}\right)\right\}\tilde{\Phi}_nD_n(y)$$
$$+\sum_{n=0}^{\infty}\frac{(1-2\eta_2)K'_md}{16}[D_{n+2}(y)+n(n-1)D_{n-2}(y)]\tilde{\Phi}_n$$
$$=\sum_{n=0}^{\infty}\frac{(1-2\eta_2)d}{4}\left[ik-K'_m\left(k^2+\frac{2n+1}{4}\right)\right]\bar{\Phi}_nD_n(y)$$
$$+\sum_{n=0}^{\infty}\frac{(1-2\eta_2)dK'_m}{16}[D_{n+2}(y)+n(n-1)D_{n-2}(y)]\bar{\Phi}_n, \tag{22}$$

$$\sum_{n=0}^{\infty}\left(-i\sigma+\frac{dK'_m}{4}\right)\left\{-\left(k^2+\frac{2n+1}{4}\right)D_n(y)+\frac{1}{4}[D_{n+2}(y)+n(n-1)D_{n-2}(y)]\right\}\bar{\Phi}_n$$
$$+\sum_{n=0}^{\infty}ik\left(\frac{1}{2}+\frac{d}{4}\right)D_n(y)\bar{\Phi}_n=\sum_{n=0}^{\infty}\frac{d}{4}\left[ik-K'_m\left(k^2+\frac{2n+1}{4}\right)\right]D_n(y)\tilde{\Phi}_n$$
$$+\sum_{n=0}^{\infty}\frac{dK'_m}{16}[D_{n+2}(y)+n(n-1)D_{n-2}(y)]\tilde{\Phi}_n \tag{23}$$

Now truncating the series (22) and (23) at $n=2$, considering the orthogonality of parabolic cylinder functions, we obtain a complex eigenvalue problem. These eigenvalues are sought out using QR methed.

III. RESULTS AND ANALYSIS

Now we will discuss the solutions of different cases.

(1) $d=0.0$

It corresponds to the case of no coupling and no condensation heating. The Eqs.(22) and (23) become

$$\left(\frac{\partial^2}{\partial x^2}+\frac{\partial^2}{\partial y^2}-\frac{y^2}{4}\right)\tilde{\Phi}+\frac{1}{2}\tilde{\Phi}_x=0, \tag{24}$$

$$\left(\frac{\partial^2}{\partial x^2}+\frac{\partial^2}{\partial y^2}\right)\overline{\Phi}_t+\frac{1}{2}\overline{\Phi}_x=0. \tag{25}$$

The eigenfrequencies corresponding to Eqs.(22) and (23) are

$$\tilde{\sigma}=\frac{-k}{2(k^2+n+\frac{1}{2})}, \qquad n=0,1,2, \tag{26}$$

$$\bar{\sigma}_0=\frac{-1}{2}\frac{k}{k^2-\frac{1}{4}}, \qquad n=0, \tag{27}$$

$$\bar{\sigma}_1=\frac{-1}{2}\frac{k}{k^2+\frac{3}{4}}, \qquad n=1, \tag{28}$$

$$\bar{\sigma}_2=\frac{-1}{2}\frac{k}{k^2+1}, \qquad n=2, \tag{29}$$

Obviously, they are all westward propagating high frequency waves, where Eq.(24) shows that the baroclinic component consists of tropical Rossby waves (Mutsuno, 1966). In the case of no interaction, the barotropical part and baroclinic part propagate in different way, just because the former is nondivergent while the latter convergent / divergent.

(2) $d=0.4, \eta_2=2.5$

Fig. 2 depicts the real part and imaginary part of the eigenvalues varying with the nondimensional wavenumber k.

From Fig. 2a, it is noticed that through the dynamical coupling and interaction between the barotropic and baroclinic components via tropical boundary layer frictional convergence, a traditional westward propagating Rossby wave now becomes eastward propagating when its wavenumber k is small, and at about $k=0.5$, this mode changes its direction and becomes

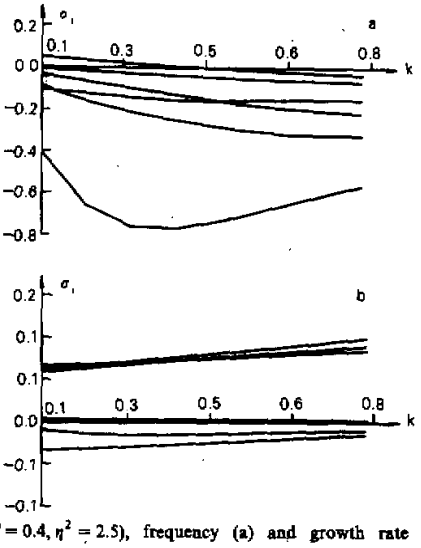

Fig. 2. Case 2 ($d=0.4, \eta^2=2.5$), frequency (a) and growth rate (b) as a function of nondimensional wavenumber k.

westward propagating again. In the meantime, there are other two eigenmodes whose phase speeds are much slower than the free Rossby waves. From Fig. 2. b, we'll see that the foregoing three eigenmodes are all instable. However, there are the other three eigenmodes whose frequencies are as high as free modes, we name them "high frequency coupled modes". Coupling has little effect on them. The causes that the eastward propagating at long wave range will be discussed later. The eastward propagating speed of tropical atmospheric 30–60 day oscillation is about 5–15 m s^{-1}, the phase speed of the eastward propagating eigenmode is also close to the observed. Besides this, there are unstable westward propagating eigenmodes, which can be used to explain the observed westward propagating of low-frequency oscillation. Knutson (1987) analyzed the longitudinal distribution and its evolution of 30–60 day band-pass filtered velocity potential, OLR and geopotential height. His results show that the westward propagation of the disturbance exists in the tropical area. Because the traditional equatorial Rossby waves are westward propagating, it is impossible to use them to explain the mainly slow eastward propagation of the 30–60 day oscillation, but in our study, CISK mechanism and the effect of convergence in tropical boundary layer have changed some of the Rossby waves' properties. These changed Rossby waves can help us explain some features of the tropical atmospheric 30–60 day oscillation.

The analysis of the observed data shows that the 30–60 day oscillation does not decay while it propagates, even tends to be intensified over the eastern Indian Ocean–western Pacific area (Rui and Wang, 1990). The fact proves the existence of instability. Our model results also show that the instability is responsible for the variation. Rui and Wang's analysis also shows that negative OLR anomaly tends to emanate away the equatorial area toward the North American and South-Eastern Pacific, suggesting the existence of intraseasonal tropical–extratropical interaction. We believe that it is caused by Rossby wave train or energy dispersion. It will be difficult by use of the CISK–Kelvin wave theories to explain the phenomenon.

Fig.3 depicts the eigenfunction structures for baroclinic and barotropic components corresponding to $k = 0.2$, $\sigma = 0.035 + 0.068i$, $t = 0.5$. We note that baroclinic part is the main, the maximum amplitude of baroclinic part is about 3–4 times as that of barotropic one, there is little phase difference between them. The convergence / divergence of meridional winds is greater than that of zonal winds, and the maximum is located near the equator. Meridional winds are antisymmetric about the equator and substantial even away from the equator. The observed data have demonstrated it. Fig.4 shows the structures of U and Φ at levels 1 and 3. Upper level flows are out of phase with lower level flow, and the ampitudes of the former are greater than those of the latter. In the vertical direction, flow fields and geopotential have a westward tilt. This characteristic may be connected with the boundary layer frictional convergence. The fact that upper level winds are greater than lower level winds shows the importance of the interaction between high-order vertical modes and boundary layer friction.

(3) $d = 0.2$, $\eta_2 = 2.5$

It is found in this case that the growth rates of unstable modes are a little smaller than those in Case (2), and have no eastward propagation even in long wave range (figures omitted). The maximum of the vertical velocity at the top of the boundary layer W_B is greater, just because d is smaller and thus the impact of the frictional convergence is also smaller.

(4) $d = 0.2$, $2 = 5.0$

This case means there is stronger convection heating. The results are similar to those

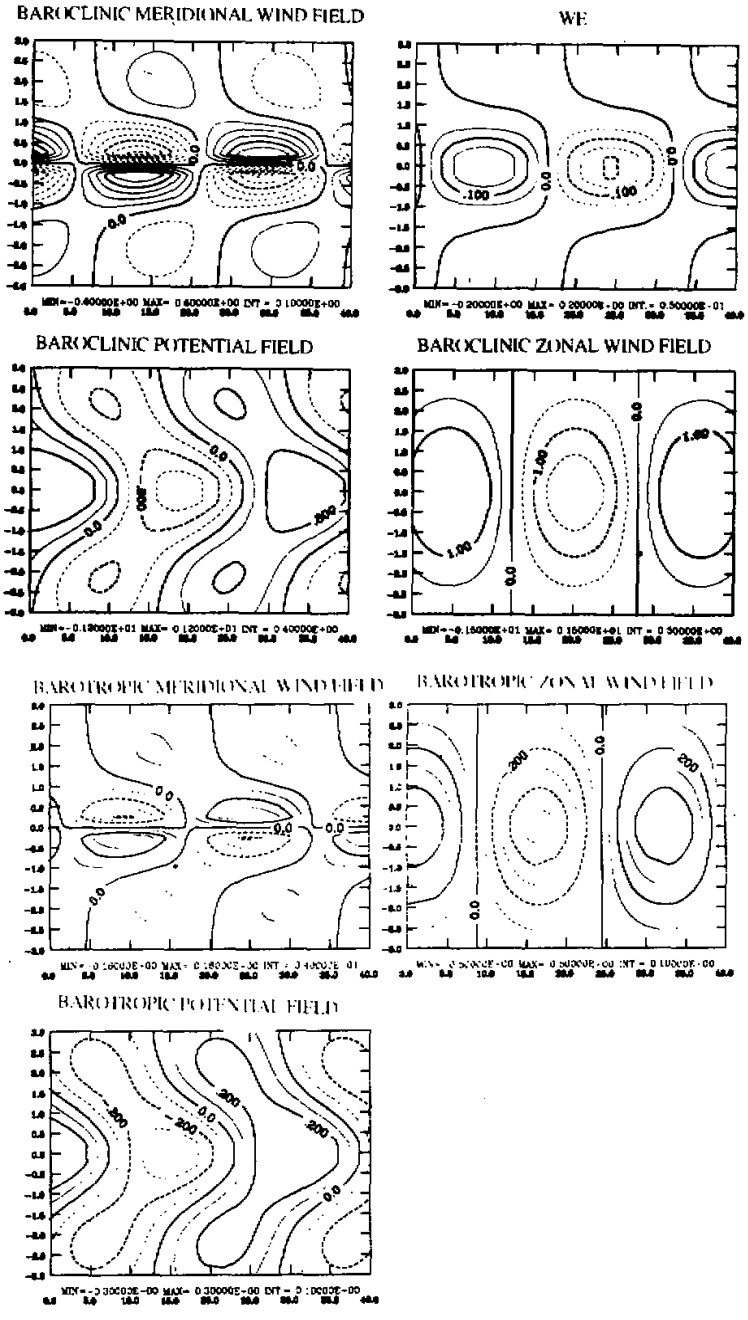

Fig. 3. Horizonal structures for baroclinic component (a) and barotropic component (b) corresponding to $k = 0.2$, $\sigma = 0.035 + 0.068i$, $t = 0.2$.

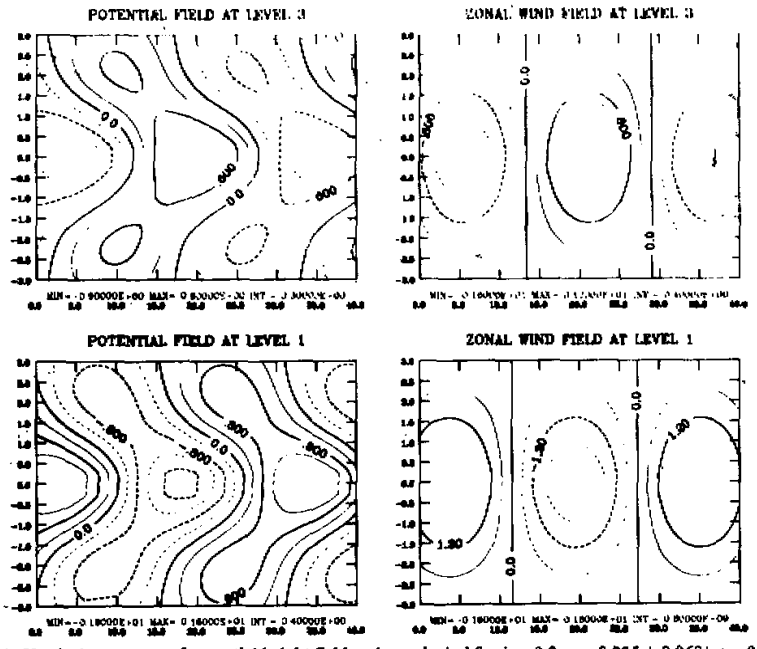

Fig. 4. Vertical structures of potential height field and zonal wind for $k = 0.2$, $\sigma = 0.035 + 0.068i$, $t = 0.2$.

shown in Fig.2, but the growth rates are greater. It can be suggested that the increment of condensation heating rate will pose more heat on the atmosphere, and enhance the growth rate of unstable modes.

(5) $d = 0.2$, $\eta_2 = 0.0$

In this case, no condensation heating exists, the distribution of real parts of eigenvalues is close to that of free Rossby wave, but imaginary parts are all negative. For this special case, the results show that the condensation heating release is a necessary condition for reproducing the modes which resemble the observed. The interaction between the barotropic and baroclinic components through the boundary convergence / divergence can not excite unstable growing modes, in the contrary, unstable decaying modes appear due to the boundary layer friction.

We also detect the instability condition of the system in the view of energy transformation. The system's energy variation can be described from Eqs.(20) and (21) as

$$\frac{\partial}{\partial t}\langle\left\{\frac{1}{2}(\nabla\bar{\Phi})^2+(\nabla\tilde{\Phi})^2+\frac{\gamma^2}{4}\tilde{\Phi}^2\right\}\rangle=-\frac{(1-2\eta_2)dK'_m}{4}\langle(\nabla\tilde{\Phi})^2\rangle-\frac{dK'_m}{4}\langle(\nabla\bar{\Phi})^2\rangle$$
$$+\frac{d}{2}\langle\nabla\tilde{\Phi}\cdot\nabla\bar{\Phi}\rangle+\frac{d\eta_2}{2}\left[\langle\tilde{\Phi}\bar{\Phi}_x\rangle+K'_m\langle\tilde{\Phi}\nabla^2\tilde{\Phi}\rangle\right], \tag{30}$$

where $\langle\ \rangle=\int_{-\infty}^{+\infty}dy\int_0^L dx$, L is zonal wavelength. It is obvious that for and $\nabla\tilde{\Phi}$ must be positively correlated, and $\eta_2 > 1/2$. In Case (5), $\bar{V}$ and $\tilde{V}$ are positively correlated, but $\bar{U}$ and $\tilde{U}$ have a little phase difference, and there is an energy sink, $-\frac{dK'_m}{4}\langle(\nabla\bar{\Phi})^2\rangle$, the ener-

gy source can not compensate for the energy sink. The total energy decays and unstable damped modes appear.

The baroclinic components are the main parts that excite the model unstability, just because the amplitudes of baroclinic components are greater than those of barotropic ones, and low–frequency waves associated with condensation heating can affect vorticity balance to maintain the baroclinic structure of the tropical atmosphere.

IV. DEPENDENCES OF THE FREQUENCY AND GROWTH RATE ON d AND η_2

It is clear that the condensation heating rate η_2 and the mixed layer depth are important to the couple modes. Fig.5 shows that the frequency (a) and growth rate(b) change with nondimensional mixed–layer depth d when nondimensional heating rate is 2.5. Only when d is greater than the critical values will the eigenmodes become unstable growth and change their propagation direction. Since d is closely related to vertical velocity at the top of the

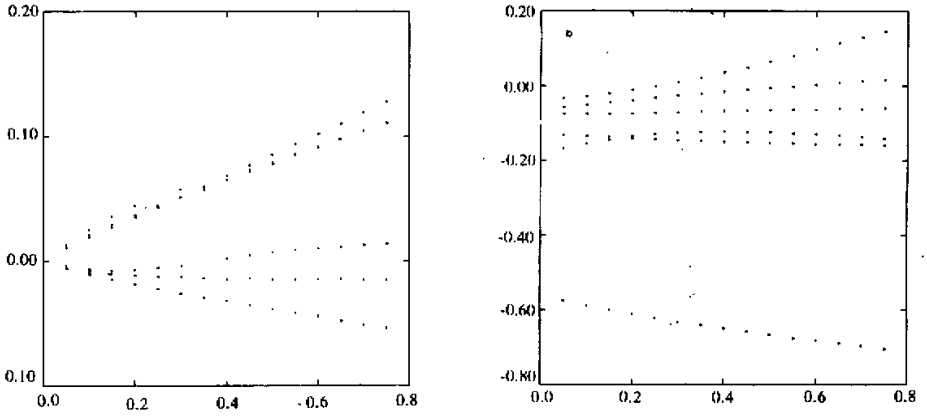

Fig. 5. The frequency (a) and growth rate (b) as a function of the nondimensional depth of mixed layer d for $\eta_2 = 2.5$.

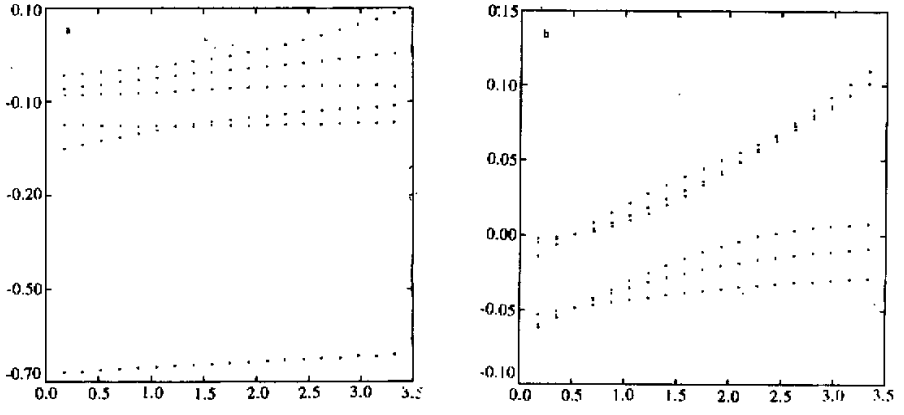

Fig. 6. The frequency (a) and growth rate (b) as a function of the nondimensional condensation rate η_2 for $d = 2.5$.

boundary layer W_B and also the convective heating, this result shows obviously that the condensation heating plays an important control role in the activities of the coupled modes.

The parameter η_2 represents the condensation heating directly, its effects on the frequency and growth rate of the coupled modes are similar to those of the parameter d (Fig. 6).

V. CONCLUSIONS AND DISCUSSIONS

In this paper, a linear quasi-geostrophic model that consists of a well-mixed layer and a two-layer free atmosphere is constructed, and the equatorial beta plane approximation is adopted, which is different from the author's previous work. Based on the analysis of instability in the model, the following conclusions are obtained.

(1) Unstable waves will be excited through the coupling and interaction between the horizontal modes and vertical modes, but only when the condensation heating is strong enough and the depth of mixed-layer is depressed enough, the unstable eastward propagating wave appears. This kind of wave resembles the observed 30–60 day oscillation in tropical atmosphere in many aspects. If there is no or not enough strong condensation heating or depressed mixed-layer, the unstable decaying wave will appear. Lau and Peng (1987) ascribed the slow propagation of the 30–60 day oscillation to the following mechanism: Kelvin wave is selected to amplify due to mobile wave-CISK mechanism, in turn the Kelvin wave leads the heat source to migrate eastward. On the left side of the heat source, new Kelvin wave is excited, and then the intraseasonal perturbation propagates eastward. The results of our study show that the intraseasonal disturbance not only depends on the impacts of eastward propagating Kelvin wave, but also Rossby wave. Hendon (1988) pointed out that CISK mechanism has great impact on the static stability of the atmosphere. In the western side of divergent field,the static rate is greater, but in the eastern region, the static rate is smaller. The fact makes perturbation develop in the eastern side. Hendon's theory on the unstable eastward propagation will be applied to explain our model results.

(2) In the past, a number of theories and numerical simulations use the Kelvin wave mode to represent the 30–60 day oscillation in the tropical atmosphere. It is well-known that Kelvin wave decays rapidly in the meridional direction. It is very difficult to use it to explain the Rossby wave train characteristics of the low-frequency oscillation. The data analysis also shows that equatorial zonal winds are often associated with the winds system in the subtropical area. Anomaly easterlies are connected with the anticyclone in the subtropical, while westerlies with the cyclone(Rui and wang, 1990). In Hendon's model, the coupling of winds in the equatorial area and cyclonic or anticyclonic cells is obvious. But the coupled structure is difficult to explain with the Kelvin wave. We think that Rossby-type mode is responsible for the formation of the foregoing cells. Of course, as pointed by Hendon,nonlinearity is also an important factor. Although some explanations of the 30–60 day oscillation are put forward, there are still a number of questions to be answered, for example, what roles does nonlinearity play in the formation and propagation of LFO ?, and can the 30–60 day oscillation be regarded as a cycle like ENSO? These questions need to be further studied later.

REFERENCES

Anderson, D. L. T., and Gill, A. E. (1975), Spin-up of a stratified ocean, with applications to upwelling, *Deep-Sea Res.*, **22**: 583–596.

Chang C. P. (1977), Viscous internal gravity waves and low-frequency oscillations in the tropics, *J. Atmos. Sci.*, **34**: 900–910.

Chao Jiping and Zhang renhe (1988), The air–sea interaction wave in the tropics and their instabilities, *Acta. Meteo. Sinica* **2:** 275–287.

Hayashi, Y. Y., and A. Sumi (1986), The 30–40 day oscillations simulated in an "Aqua Pinet" model, *J. Meteor. Soc. Japan,* **144:** 451–467.

Hendon, G. H. (1988), A simple model of the 40–50 day oscillation, *J. Atmos. Sci.,* **45:** 569–584.

Knutson, T. R., and K. M. Weickman (1987), 30–60 day atmospheric oscillation composite life cycles of convection and circulation anomalies, *Mon. Wea. Rev.* **115:** 1407–1436.

Lau, K. –M., and L. Peng (1987), Origin of the low–frequency (intraseasonal) oscillation in the tropical atmosphere, Part I: Basic theory, *J. Atmos. Sci.,* **44:** 950–972.

Li Chongyin (1985), Actions of summer monsoon troughs (ridges) and tropical cyclones over South Asia and the moving CISK mode, *Scientia Sinica* (B), **28:** 1197–1207.

Liu Shikuo and Wang Jiyong (1990), A baroclinic semi–geostrophic model using the wave–CISK theory and low–frequency oscillation, *Acta Meteor. Sinica,* **4:** 576–585.

Madden, R. A., and P. R. Julian (1971), Detection of 40–50 day oscillation in the zonal wind in the tropical Pacific, *J. Atmos. Sci.,* **28:** 702–708.

————(1972), Description of global circulation cells in the tropics with 40–50 day period, *J. Atmos. Sci.,* **29:** 1109–1123.

Matsuno, T. (1966), Quasi–geostrophic motions in the equatorial area, *J. Meteor. Soc. Japan,* **44:** 25–43.

Rui, H., and B,. Wang (1090), Development characteristics and dynamics structure of tropical intraseasonal convective anomalies, *J. Atmos. Sci.,* **47:** 357–379.

Swinbank, R., T. N. Palmer and M. K. Davey (1988), Numerical simulation of Madden and Julian oscillation, *J. Atmos. Sci.,* **45:** 774–78.

Takahashi, M. (1987), A theory of slow phase speed of the intraseasonal oscillation using the wave CISK, *J. Meteor. Soc. Japan,* **65:** 43–49.

Wang, B. (1988), Dynamics of tropical low–frequency waves: an analysis of the moist Kelvin wave, *J. Atmos. Sci.,* **45:** 2051–2065.